1-1-2007

Quasi-Orthogonal Space-Time-Frequency Codes in MB-OFDM UWB Communications

L. C. Tran
University of Lübeck, tran@isip.uni-luebeck.de

A. Mertins
University of Lübeck, mertins@isip.uni-luebeck.de

Tadeusz A. Wysocki
University of Nebraska-Lincoln, twysocki2@unl.edu

Quasi-Orthogonal Space-Time-Frequency Codes in MB-OFDM UWB Communications

L. C. Tran, A. Mertins
Institute for Signal Processing
University of Lübeck, Germany
Email: {tran,mertins}@isip.uni-luebeck.de

T. A. Wysocki
School of Elec. Comp. & Telecomm. Eng.
University of Wollongong, Australia
Email: wysocki@uow.edu.au

***Abstract*— The paper examines the implementation of Quasi-Orthogonal Space-Time-Frequency Codes (QOSTFCs) to increase data rates and error performance in recently proposed STFC Multiband OFDM Ultra Wideband (MB-OFDM UWB) communications systems. It is shown that, an order-4 QOSTFC not only can provide the full rate, but also may provide significantly better error performance, compared to the conventional MB-OFDM (without STFCs), and considerably better error performance, compared to order-4, orthogonal STFC MB-OFDM, without increasing the total transmission power.**

I. Introduction

Multiband Orthogonal Frequency Division Multiplexing Ultra-Wideband (MB-OFDM UWB) communications technology [1] is a potential candidate for short range communications (up to 10 meters) with a very high rate (480 Mbps), low power consumption and emission, and at low cost. On the other hand, Multiple Input Multiple Output (MIMO) systems using multiple transmit (Tx) antennas and/or multiple receive (Rx) antennas have recently been intensively examined, because they can provide potentially a very high system capacity, which in various cases grows linearly with the maximum number of Tx and Rx antennas, without any increase of the total transmission power [2], [3]. Space-Time Codes (STCs) [4], [5], [6], [7], [8] are the codes designed for the use of MIMO systems.

Intuitively, the combination of the emerging technologies MB-OFDM UWB, MIMO, and STCs will provide a significant improvement in the maximum achievable communications range, bit error performance, system capacity, and data rate. While the combination of OFDM, MIMO and STCs in the form of Space-Time-Frequency Codes (STFCs) in MIMO-OFDM systems (referred to as STFC-MIMO-OFDM systems) has been well examined in the literature, such as [9], [10], [11], [12], [13], the combination of MB-OFDM UWB, MIMO, and STCs has been almost unexplored with few papers examining this issue [14], [15], [16], [17]. There are two main differences between channels' characteristics in conventional OFDM systems and in MB-OFDM UWB ones. First, channels in the conventional OFDM system are much less dispersive than those in the MB-OFDM UWB system because the latter has much larger bandwidth. Second, channel coefficients in the conventional OFDM system are usually considered to be Rayleigh distributed, while those in the MB-OFDM UWB system are log-normally distributed [18]. Therefore, the systems incorporating MB-OFDM UWB, MIMO, and STCs must be more specifically analyzed, though there exist some similarities between them and the conventional STFC-MIMO-OFDM systems.

The combination between MB-OFDM UWB systems with Space-Time Block Codes (STBCs) has been mentioned in [14] for only 2 Tx antennas, i.e. the Alamouti code [4]. In [15], the authors proposed a general framework to analyze the performance of MB-OFDM MIMO UWB systems regardless of specific coding schemes. They quantified the performance of the MB-OFDM MIMO UWB in case of Nakagami frequency-selective fading channels. In [19], we proposed the STFC MB-OFDM UWB system for any number of Tx/Rx antennas. We followed an approach to examine the performance of STFC MB-OFDM UWB systems, independently of the existing works. Particularly, we modified Tarokh's proof mentioned in [5] for the conventional wireless STC MIMO communications to quantify the diversity and coding gains of the proposed STFC MB-OFDM UWB system in the log-normal distribution case [20]. Our analysis was based closely on WiMedia's MB-OFDM UWB physical layer specifications [1] and the IEEE 802.15.3a UWB channel model [18]. We discovered that the maximum achievable diversity gain of the proposed STFC MB-OFDM UWB system is the product of the numbers of Tx and Rx antennas and the FFT size.

One disadvantage of STFCs constructed based directly on complex orthogonal STBCs (CO STBCs) as mentioned in [19] is the reduced code rate when the number of Tx antennas is greater than two. It is well known that CO STBCs for more than two Tx antennas cannot provide the full rate. To overcome this disadvantage, in [21], the author proposed quasi-orthogonal STBCs (QOSTBCs) for four and eight Tx antennas providing higher data rates than the conventional CO STBCs for the same order, while they still can provide a large (but not full) diversity. In QOSTBCs, the orthogonality between columns (or rows) is partially relaxed, allowing for more symbols to be transmitted in the code blocks.

The idea of QOSTBCs can definitely be further extended for STFC MB-OFDM UWB systems. Therefore, in this paper, we consider the application of Quasi-Orthogonal STFCs (QOSTFCs), which usually have higher code rates than orthogonal STFCs (OSTFCs) of the same order, in the proposed STFC

MB-OFDM UWB system. In particular, we analyze the error performance of the half-diversity, full-rate, order-4 QOSTFC, which is constructed based on the QOSTBC proposed in [21] for conventional wireless MIMO STBC systems. The performance of the QOSTFC will be compared to that of an orthogonal, full-diversity, rate-3/4, order-4 STFC, and that of the conventional MB-OFDM (without STFCs). It will be shown that, although only half diversity can be achieved, QOSTFCs may still provide better error performance over OSTFCs of the same order, without any increase of the total transmission power.

The paper is organized as follows. In Section II, we review the specifications of our STFC MB-OFDM system proposed in [19]. Section III analyzes the feasibility of the deployment of order-4 STFCs in the STFC MB-OFDM system, and analyzes the decoding metrics for an order-4 OSTFC and an order-4 QOSTFC. In Section IV, various simulation results in the modulation schemes QPSK, 16-QAM and Dual Carrier Modulation (DCM) [22] are shown to verify our analysis. Conclusions are drawn in Section V.

II. STFC MB-OFDM UWB System

The diagram of the proposed STFC MB-OFDM UWB system with the notations of signals at the considered reference points is depicted in Fig. 1. The system consists of M Tx antennas and N Rx antennas. Assuming that the transmitted STFC is the following matrix

$$\mathbf{S} = \{\bar{\mathbf{s}}_{t,m}\}_{T\times M} \quad (1)$$

where T denotes the number of MB-OFDM symbol time slots required to transmit the whole STFC block. Structures of $\mathbf{S}$ are the same as those of CO STBCs in conventional wireless STBC MIMO systems [4], [7], [6], [23], [24], except for that each element $\bar{\mathbf{s}}_{t,m}$ is not a complex number, but defined as a column vector $\bar{\mathbf{s}}_{t,m} = [s_{t,m,1}, s_{t,m,2}, \ldots, s_{t,m,N_{fft}}]^T$. The vectors $\bar{\mathbf{s}}_{t,m}$ are the original transmitted data before IFFT. The symbols $s_{t,m,k}$ are drawn from a QPSK or DCM constellation. The superscript T denotes the transposition operation.

Elements $\bar{\mathbf{s}}_{t,m}$ in each row of $\mathbf{S}$ are transmitted simultaneously through M Tx antennas in the same frequency band, while different rows of $\mathbf{S}$ might be transmitted in different frequency bands, following a certain Time-Frequency Code (TFC). Different TFCs (transmitted RF patterns) are described in more details in [1].

Denote $\mathcal{X} = \{\bar{\mathbf{x}}_{OFDM,t,m}\}_{T\times M}$ to be the matrix whose elements are the N_{fft}-point IFFTs of the respective element in $\mathbf{S}$, then

$$\mathcal{X} = \{IFFT\{\bar{\mathbf{s}}_{t,m}\}\}_{T\times M} \quad (2)$$
$$= \{\bar{\mathbf{x}}_{OFDM,t,m}\}_{T\times M}. \quad (3)$$

The symbols $\bar{\mathbf{x}}_{OFDM,t,m}$ are referred to as MB-OFDM symbols. Further, denote $\mathcal{X}_{\mathbf{ZP}} = \{\bar{\mathbf{x}}_{ZP,t,m}\}_{T\times M}$ to be the matrix whose elements are the respective element in $\mathcal{X}$ appended by a ZPS of 37 zeros. Clearly, $\bar{\mathbf{x}}_{OFDM,t,m}$ is the transmitted MB-OFDM symbol before Zero Padding (ZP), while $\bar{\mathbf{x}}_{ZP,t,m}$ is the actual transmitted symbol after ZP. Denote

TABLE I

Numbers of Multipaths Np_{10dB}, $Np_{85\%}$, and $\bar{N}_p$ [18].

	CM 1	CM 2	CM 3	CM 4
Np_{10dB}	12.5	15.3	24.9	41.2
$Np_{85\%}$	20.8	33.9	64.7	123.3
$\bar{N}_p$	287.9	739.5	1463.7	3905.5

$$\bar{\mathbf{h}}_{m,n} = \left[\ h_{m,n,1} \quad h_{m,n,2} \quad \ldots \quad h_{m,n,L_{m,n}}\ \right]^T \quad (4)$$

to be the channel vector between the m-th Tx and n-th Rx antennas, for $m = 1, \ldots, M, n = 1, \ldots, N$, where the channel coefficients $h_{m,n,l}$ of the l-th path, $l = 1, \ldots, L_{m,n}$, in this channel are modeled as independent *log-normally* distributed random variables (RVs). Let $L_{max} = \max\{L_{m,n}\}$, for $m = 1, \ldots, M, n = 1, \ldots, N$. Denote the MB-OFDM UWB channel coefficient matrix as

$$\mathbf{H} = \{\bar{\mathbf{h}}_{m,n,ZP}\}_{M\times N} \quad (5)$$

where the vector $\bar{\mathbf{h}}_{m,n,ZP}$ is created from the corresponding channel vector $\bar{\mathbf{h}}_{m,n}$ by adding zeros to have the length L_{max}.

At the transmission of the t-th MB-OFDM symbol, the received signal at the n-th Rx antenna is calculated as

$$\bar{\mathbf{r}}_{ZP,t,n} = \sum_{m=1}^{M} \left(\bar{\mathbf{x}}_{ZP,t,m} \otimes \bar{\mathbf{h}}_{m,n}\right) + \bar{\mathbf{n}}_{t,n} \quad (6)$$

where $\otimes$ denotes the *linear convolution*. The elements of noise vector $\bar{\mathbf{n}}_{t,n}$ are considered to be independent complex Gaussian RVs.

A. Theoretical Analysis

In this section, we first analyze the proposed system with the theoretical assumption that the maximum number of multipaths $L_{m,n}$, for $m = 1, \ldots, M, n = 1, \ldots, N$, is $(N_{ZPS} + 1)$, where N_{ZPS} denotes the length of the ZPS. Instead of inserting a CP at the transmitter and discarding the CP at the receiver as in a conventional OFDM system, in MB-OFDM system, a ZPS of a length N_{ZPS} is appended to each symbol $\bar{\mathbf{x}}_{OFDM,t,m}$ at the transmitter to create a transmitted symbol $\bar{\mathbf{x}}_{ZP,t,m}$. At the receiver, an Overlap-And-Add Operation (OAAO) must be performed before FFT. OAAO means that the N_{ZPS} samples of a received symbol $\bar{\mathbf{r}}_{ZP,t,n}$, ranging from $(N_{fft}+1)$ to $(N_{fft}+N_{ZPS})$, are added to the beginning of that received symbol. Then the first N_{fft} samples of the resulting symbol will be used to decode the transmitted symbol. These N_{fft} samples are exactly equivalent to the *circular convolution* of the transmitted OFDM symbol (before ZP) $\bar{\mathbf{x}}_{OFDM,t,m}$ with the channel $\bar{\mathbf{h}}_{m,n}$. This exact equivalence is due to the fact that, if a ZPS of a length N_{ZPS} is used, the greatest multipath tolerance of the system is $(N_{ZPS} + 1)$. Consequently, from the theoretical viewpoint, the number of multipaths (the length of vectors $\bar{\mathbf{h}}_{m,n}$) must not exceed $(N_{ZPS} + 1)$.

As a result, after performing OAAO for the received signal $\bar{\mathbf{r}}_{ZP,t,n}$ in (6), and then taking the first N_{fft} resulting samples,

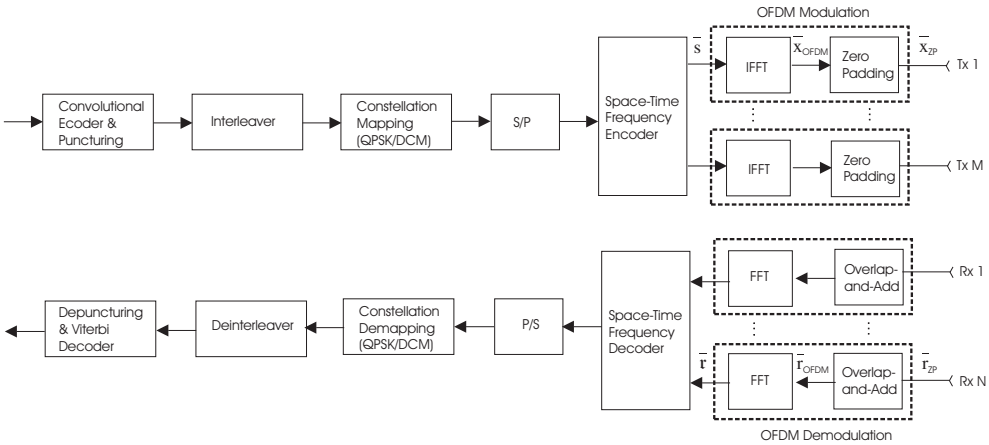

Fig. 1. Structural diagram of the proposed STFC MB-OFDM UWB systems.

denoted as $\bar{\mathbf{r}}_{OFDM,t,n}$, the following equation is deduced

$$\bar{\mathbf{r}}_{OFDM,t,n} = \sum_{m=1}^{M} \bar{\mathbf{x}}_{OFDM,t,m} * \bar{\mathbf{h}}_{m,n} + \bar{\mathbf{n}}_{t,n} \quad (7)$$

where $*$ denotes the *cyclic convolution* or *circular convolution*. For the circular convolution, we have the following property

$$\begin{aligned} \bar{\mathbf{x}}_{OFDM,t,m} * \bar{\mathbf{h}}_{m,n} &= IFFT\{FFT\{\bar{\mathbf{x}}_{OFDM,t,m}\} \bullet \\ &\quad FFT\{\bar{\mathbf{h}}_{m,n}\}\} \\ &= IFFT\{\bar{\mathbf{s}}_{t,m} \bullet \bar{\mathfrak{h}}_{m,n}\} \end{aligned} \quad (8)$$

where $\bullet$ denotes the element-wise or Hadamard product, and $\bar{\mathfrak{h}}_{m,n}$ is the N_{fft}-point FFT of the channel vector $\bar{\mathbf{h}}_{m,n}$, i.e.

$$\bar{\mathfrak{h}}_{m,n} = FFT\{\bar{\mathbf{h}}_{m,n}\} \quad (9)$$

We denote $\bar{\mathfrak{h}}_{m,n} = \begin{bmatrix} \hbar_{m,n,1} & \hbar_{m,n,2} & \dots & \hbar_{m,n,N_{fft}} \end{bmatrix}^T$.

After going through the FFT block at the receiver, the received signal becomes

$$FFT\{\bar{\mathbf{r}}_{OFDM,t,n}\} = \sum_{m=1}^{M} \bar{\mathbf{s}}_{t,m} \bullet \bar{\mathfrak{h}}_{m,n} + FFT\{\bar{\mathbf{n}}_{t,n}\} \quad (10)$$

Denote

$$\bar{\mathfrak{r}}_{t,n} = \begin{bmatrix} \mathfrak{r}_{t,n,1} & \mathfrak{r}_{t,n,2} & \dots & \mathfrak{r}_{t,n,N_{fft}} \end{bmatrix}^T = FFT\{\bar{\mathbf{r}}_{t,n}\}$$

and

$$\bar{\mathfrak{n}}_{t,n} = \begin{bmatrix} \mathfrak{n}_{t,n,1} & \mathfrak{n}_{t,n,2} & \dots & \mathfrak{n}_{t,n,N_{fft}} \end{bmatrix}^T = FFT\{\bar{\mathbf{n}}_{t,n}\}.$$

Then (10) can be rewritten as follows

$$\bar{\mathfrak{r}}_{t,n} = \sum_{m=1}^{M} \bar{\mathbf{s}}_{t,m} \bullet \bar{\mathfrak{h}}_{m,n} + \bar{\mathfrak{n}}_{t,n}. \quad (11)$$

Recall that $\bar{\mathbf{s}}_{t,n}$ is the original QPSK or DCM transmitted signal (before IFFT).

Denote $\mathcal{H} = \{\bar{\mathfrak{h}}_{m,n}\}_{M\times N}$ to be the matrix whose elements are the N_{fft}-point FFTs of the respective element in the channel coefficient matrix $\mathbf{H}$. Further, denote $\mathbf{R} = \{\bar{\mathbf{r}}_{OFDM,t,n}\}_{T\times N}$ to be the received signal matrix, $\mathcal{R} = \{\bar{\mathfrak{r}}_{t,n}\}_{T\times N}$ to be the received signal matrix after FFT, and $\mathcal{N} = \{\bar{\mathfrak{n}}_{t,n}\}_{T\times N}$ to be the noise matrix.

We can rewrite (11) in matrix form as follows

$$\mathcal{R} = \mathbf{S} \circ \mathcal{H} + \mathcal{N} \quad (12)$$

where we define the multiplication operation $\circ$ between $\mathbf{S}$ and $\mathcal{H}$ as that the (t,n)-th element of the resulting matrix is a N_{fft}-length column vector $\sum_{m=1}^{M} \bar{\mathbf{s}}_{t,m} \bullet \bar{\mathfrak{h}}_{m,n}$.

From (12), we can realize that there exists a similarity between the mathematical model of the STFC MB-OFDM UWB system and that of the conventional wireless STC MIMO system [4], [7], [25]. The only difference between the two mathematical models is that elements in each matrix are numbers in the conventional STC MIMO system, while they are N_{fft}-length column vectors in the STFC MB-OFDM UWB system.

Because the vector elements in $\mathbf{S}$ will be transformed via IFFT to generate MB-OFDM symbols with N_{fft} subcarriers, we refer $\mathbf{S}$ to as a Space-Time-Frequency Code.

B. Realistic Channel Condition

The error performance of the proposed system with realistic UWB channel conditions is inferior, compared to the theoretical performance, due to the following two main reasons.

In theory, the length of CP or ZPS must be longer than the longest multipath in an OFDM-based system to turn the linear convolution between the transmitted signal and the channel vector into the circular convolution. However, in practice, the multipath length is very likely to exceed the length of CP or ZPS. This is especially true in MB-OFDM UWB systems where the average number of multipaths $\bar{N}_p$ is usually much bigger than $N_{ZPS} = 37$ (see Table I). The transition from (6) to (11) is an approximation, due to the fact that the circular convolution in (8) is approximately, but not exactly equal to the first N_{fft} samples achieved by the OAAO of the linear convolution $\bar{\mathbf{x}}_{ZP,t,m} \otimes \bar{\mathbf{h}}_{m,n}$ in (6). The energy of multipath components within the ZPS window will be captured, while the multipath components outside this window may be considered as interferences for the received

signals. Eq. (6) represents the real received signals at the Rx antennas, while (11) shows the realistic concept used at the STFC decoder to decode the original transmitted signals. By calculating the received signals $\bar{\mathbf{r}}_{ZP,t,n}$ with the full impact of long multipath channels (with the linear convolution) based on (6), and decoding signals based on (11), i.e. based on the circular convolution, we can simulate the performance of the proposed system, which is closed to the realistic performance of the system. Thereby, we can find out how the multipath channels actually impact on the system performance.

On the other hand, for a channel vector $\bar{\mathbf{h}}_{m,n} = \begin{bmatrix} h_{m,n,1} & h_{m,n,2} & \dots & h_{m,n,L_{m,n}} \end{bmatrix}^T$, we always have the following property for the N_{fft}-point FFT operation

$$FFT\{\bar{\mathbf{h}}_{m,n}\} = FFT\{\begin{bmatrix} h_{m,n,1} & \dots & h_{m,n,N_{fft}} \end{bmatrix}^T\} \tag{13}$$

when the length $L_{m,n}$ of the vector is not smaller than N_{fft}. This means that, by taking the FFT of the received signals with a *limited* FFT size N_{fft}, and decoding signals based on (11), the N_{fft}-point FFT operation truncates the impact of a long vector $\bar{\mathbf{h}}_{m,n}$ to the length of N_{fft}. Therefore, the higher N_{fft} is, the closer the approximation between the linear convolution and the circular convolution is, and thus the better the system performance is. However, FFT and IFFT blocks significantly decide the complexity and the cost of transmitter and receiver. As a result, there must be a suitable compromise between the cost/complexity and the system performance.

III. Order-4 STFCs and Decoding Metrics

If the code rate of a STFC is defined as the ratio of the number of transmitted MB-OFDM symbols and the number of time slots required to transmit the whole block of the code, it is well known that the Alamouti code

$$\mathbf{S_2} = \begin{bmatrix} \bar{\mathbf{s}}_1 & \bar{\mathbf{s}}_2 \\ -\bar{\mathbf{s}}_2^* & \bar{\mathbf{s}}_1^* \end{bmatrix} \tag{14}$$

can provide a full rate for two Tx antennas, while higher-order codes for more than two Tx antennas cannot provide the full rate. However, they can still provide a higher diversity order than the Alamouti STFC. As a result, the higher-order codes can provide better error performance without any increase of the total transmission power. Therefore, the implementation of higher-order STFCs for multiple Tx/Rx antennas in STFC MB-OFDM UWB communications is still of our interest.

To avoid the spatial correlation between Tx and/or Rx antennas, the antennas should be located by the multiples of $\lambda/2$, where λ is the wavelength, apart from each other. Let us consider the case of order-4 STFCs (4 Tx antennas are required) for instance. We assume that Tx antennas are separate from one another by $\lambda/2$, which is in the range 14.2-48.4 mm for the UWB frequency range 3.1-10.6 GHz, then the length of UWB devices locating 4 Tx antennas should be about 4.3-14.5 cm. Clearly, this length is the typical length of wireless devices, such as wireless access points or routers. Thus it can be stated that the application of 4 Tx antennas is feasible in STFC MB-OFDM UWB communications, because devices work at a very high center frequency.

From (12), the ML decoding expression can be derived in the most general form as follows

$$\{\bar{\mathbf{s}}_{dec,t,m}\} = \arg\min_{\{\bar{\mathbf{s}}_{t,m}\}} \| \mathcal{R} - \mathbf{S} \circ \mathcal{H} \|_F^2 \tag{15}$$

where $\| \ . \ \|_F$ denotes the Frobenius norm. This decoding metric is too complicated to be performed if $\mathbf{S}$ has arbitrary structures. However, if $\mathbf{S}$ are completely orthogonal (i.e. orthogonal STFCs) or partially orthogonal (i.e. QOSTFCs), the orthogonality of $\mathbf{S}$ is preserved for the MB-OFDM symbols $\bar{\mathbf{s}}_{t,m}$ transmitted inside the code block $\mathbf{S}$. As a result, each MB-OFDM symbol (for orthogonal STFCs) $\bar{\mathbf{s}}_{t,m}$, or some MB-OFDM symbols (for QOSTFCs) can be decoded separately, rather than jointly. The decoding metrics for the MB-OFDM symbols $\bar{\mathbf{s}}_{t,m}$ can be easily found, based on those decoding metrics for the respective CO STBC or QOSTBC of $\mathbf{S}$, with slight modifications. Furthermore, each data point among $N_D = 100$ data sub-carriers within a MB-OFDM symbol $\bar{\mathbf{s}}_{t,m}$ (several data points for QOSTFCs) can also be decoded separately, rather than the whole N_D data in a MB-OFDM symbol $\bar{\mathbf{s}}_{t,m}$ are decoded simultaneously. Thus the decoding process is relatively simple.

We consider here the orthogonal, rate-3/4, full diversity, order-4 STFC S_{4a}, which is constructed based on the code proposed in [26] for conventional wireless MIMO STBC systems

$$\mathbf{S_{4a}} = \begin{bmatrix} \bar{\mathbf{s}}_1 & \bar{\mathbf{s}}_2 & \bar{\mathbf{s}}_3 & 0 \\ -\bar{\mathbf{s}}_2^* & \bar{\mathbf{s}}_1^* & 0 & \bar{\mathbf{s}}_3 \\ -\bar{\mathbf{s}}_3^* & 0 & \bar{\mathbf{s}}_1^* & -\bar{\mathbf{s}}_2 \\ 0 & -\bar{\mathbf{s}}_3^* & \bar{\mathbf{s}}_2^* & \bar{\mathbf{s}}_1 \end{bmatrix} \tag{16}$$

and the full rate, half diversity, order-4 QOSTFC S_{4b}, which is constructed based on the QOSTBC proposed in [21]

$$\mathbf{S_{4b}} = \begin{bmatrix} \bar{\mathbf{s}}_1 & \bar{\mathbf{s}}_2 & \bar{\mathbf{s}}_3 & \bar{\mathbf{s}}_4 \\ -\bar{\mathbf{s}}_2^* & \bar{\mathbf{s}}_1^* & -\bar{\mathbf{s}}_4^* & \bar{\mathbf{s}}_3^* \\ -\bar{\mathbf{s}}_3^* & -\bar{\mathbf{s}}_4^* & \bar{\mathbf{s}}_1^* & \bar{\mathbf{s}}_2^* \\ \bar{\mathbf{s}}_4 & -\bar{\mathbf{s}}_3 & -\bar{\mathbf{s}}_2 & \bar{\mathbf{s}}_1 \end{bmatrix}. \tag{17}$$

The columns ν_i, for $i = 1, \dots 4$, of S_{4b} are orthogonal, except for the pairs $\langle \nu_1, \nu_4 \rangle$ and $\langle \nu_2, \nu_3 \rangle$. Clearly, the orthogonality of S_{4b} (thus the diversity) is partially released to achieve the full rate. Each MB-OFDM symbol can be decoded separately for the code S_{4a}, while a pair of MB-OFDM symbols must be decoded at a time for the code S_{4b}. The decoding metrics of MB-OFDM symbols in the two codes can be easily found based on the decoding metrics of the respective STBC and QOSTBC.

First, we consider a MISO system (1 Rx antenna) using PSK or QAM modulation schemes. For simplicity, we denote the channel coefficient vectors between the Tx antennas and the Rx antenna to be $\bar{\mathfrak{h}}_m$, for $m = 1, \dots, 4$. The decoding metrics of the MB-OFDM symbols are presented in Tables II and III, where $.\hat{}$ denotes the element-wise power operation, $\bar{\mathbf{1}}$ denotes a column vector of length N_D, whose elements are all 1, and the N_D-dimensional complex space $\mathcal{C}^{N_D}$ denotes all potential possibilities that the vector $\bar{\mathbf{s}}$ can take.

TABLE II

DECODING METRICS FOR $\mathbf{S_{4a}}$ WITH PSK OR QAM MODULATIONS.

Symbol	Decoding Metric
$\bar{\mathbf{s}}_1$	$\arg\min_{\bar{\mathbf{s}}\in\mathcal{C}^{N_D}} \parallel \big[\big\vert(\bar{\mathfrak{h}}_2 \bullet \bar{\mathfrak{r}}_2^* + \bar{\mathfrak{h}}_3 \bullet \bar{\mathfrak{r}}_3^* + \bar{\mathfrak{h}}_1^* \bullet \bar{\mathfrak{r}}_1 +$ $\bar{\mathfrak{h}}_4^* \bullet \bar{\mathfrak{r}}_4) - \bar{\mathbf{s}}\big\vert.\hat{}\,2 + (-\bar{\mathbf{1}} + \sum_{m=1}^{4} \vert\bar{\mathfrak{h}}_m\vert.\hat{}\,2) \bullet (\vert\bar{\mathbf{s}}\vert.\hat{}\,2)\big] \parallel_F^2$
$\bar{\mathbf{s}}_2$	$\arg\min_{\bar{\mathbf{s}}\in\mathcal{C}^{N_D}} \parallel \big[\big\vert(-\bar{\mathfrak{h}}_2^* \bullet \bar{\mathfrak{r}}_1 - \bar{\mathfrak{h}}_4^* \bullet \bar{\mathfrak{r}}_3 - \bar{\mathfrak{h}}_1 \bullet \bar{\mathfrak{r}}_2^* +$ $\bar{\mathfrak{h}}_3 \bullet \bar{\mathfrak{r}}_4^*) - \bar{\mathbf{s}}\big\vert.\hat{}\,2 + (-\bar{\mathbf{1}} + \sum_{m=1}^{4} \vert\bar{\mathfrak{h}}_m\vert.\hat{}\,2) \bullet (\vert\bar{\mathbf{s}}\vert.\hat{}\,2)\big] \parallel_F^2$
$\bar{\mathbf{s}}_3$	$\arg\min_{\bar{\mathbf{s}}\in\mathcal{C}^{N_D}} \parallel \big[\big\vert(-\bar{\mathfrak{h}}_1 \bullet \bar{\mathfrak{r}}_3^* - \bar{\mathfrak{h}}_2 \bullet \bar{\mathfrak{r}}_4^* + \bar{\mathfrak{h}}_3^* \bullet \bar{\mathfrak{r}}_1 +$ $\bar{\mathfrak{h}}_4^* \bullet \bar{\mathfrak{r}}_2) - \bar{\mathbf{s}}\big\vert.\hat{}\,2 + (-\bar{\mathbf{1}} + \sum_{m=1}^{4} \vert\bar{\mathfrak{h}}_m\vert.\hat{}\,2) \bullet (\vert\bar{\mathbf{s}}\vert.\hat{}\,2)\big] \parallel_F^2$

TABLE III

DECODING METRICS FOR $\mathbf{S_{4b}}$ WITH PSK OR QAM MODULATIONS.

Symbols	Decoding Metric
$(\bar{\mathbf{s}}_1, \bar{\mathbf{s}}_4)$	$\arg\min_{\bar{\mathbf{s}}_1,\bar{\mathbf{s}}_4\in\mathcal{C}^{N_D}} \parallel (\sum_{m=1}^{4} \vert\bar{\mathfrak{h}}_m\vert.\hat{}\,2) \bullet (\vert\bar{\mathbf{s}}_1\vert.\hat{}\,2 + \vert\bar{\mathbf{s}}_4\vert.\hat{}\,2)$ $+2Real[(-\bar{\mathfrak{h}}_1 \bullet \bar{\mathfrak{r}}_1^* - \bar{\mathfrak{h}}_2^* \bullet \bar{\mathfrak{r}}_2 - \bar{\mathfrak{h}}_3^* \bullet \bar{\mathfrak{r}}_3 - \bar{\mathfrak{h}}_4 \bullet \bar{\mathfrak{r}}_4^*) \bullet \bar{\mathbf{s}}_1]+$ $+2Real[(-\bar{\mathfrak{h}}_4 \bullet \bar{\mathfrak{r}}_1^* + \bar{\mathfrak{h}}_3^* \bullet \bar{\mathfrak{r}}_2 + \bar{\mathfrak{h}}_2^* \bullet \bar{\mathfrak{r}}_3 - \bar{\mathfrak{h}}_1 \bullet \bar{\mathfrak{r}}_4^*) \bullet \bar{\mathbf{s}}_4]+$ $+2Real[(\bar{\mathfrak{h}}_1 \bullet \bar{\mathfrak{h}}_4^* - \bar{\mathfrak{h}}_2^* \bullet \bar{\mathfrak{h}}_3 - \bar{\mathfrak{h}}_2 \bullet \bar{\mathfrak{h}}_3^* + \bar{\mathfrak{h}}_1^* \bullet \bar{\mathfrak{h}}_4) \bullet \bar{\mathbf{s}}_1 \bullet \bar{\mathbf{s}}_4^*] \parallel_F^2$
$(\bar{\mathbf{s}}_2, \bar{\mathbf{s}}_3)$	$\arg\min_{\bar{\mathbf{s}}_2,\bar{\mathbf{s}}_3\in\mathcal{C}^{N_D}} \parallel (\sum_{m=1}^{4} \vert\bar{\mathfrak{h}}_m\vert.\hat{}\,2) \bullet (\vert\bar{\mathbf{s}}_2\vert.\hat{}\,2 + \vert\bar{\mathbf{s}}_3\vert.\hat{}\,2)$ $+2Real[(-\bar{\mathfrak{h}}_2 \bullet \bar{\mathfrak{r}}_1^* + \bar{\mathfrak{h}}_1^* \bullet \bar{\mathfrak{r}}_2 - \bar{\mathfrak{h}}_4^* \bullet \bar{\mathfrak{r}}_3 + \bar{\mathfrak{h}}_3 \bullet \bar{\mathfrak{r}}_4^*) \bullet \bar{\mathbf{s}}_2]+$ $+2Real[(-\bar{\mathfrak{h}}_3 \bullet \bar{\mathfrak{r}}_1^* - \bar{\mathfrak{h}}_4^* \bullet \bar{\mathfrak{r}}_2 + \bar{\mathfrak{h}}_1^* \bullet \bar{\mathfrak{r}}_3 + \bar{\mathfrak{h}}_2 \bullet \bar{\mathfrak{r}}_4^*) \bullet \bar{\mathbf{s}}_3]+$ $+2Real[(\bar{\mathfrak{h}}_2 \bullet \bar{\mathfrak{h}}_3^* - \bar{\mathfrak{h}}_1^* \bullet \bar{\mathfrak{h}}_4 - \bar{\mathfrak{h}}_1 \bullet \bar{\mathfrak{h}}_4^* + \bar{\mathfrak{h}}_2^* \bullet \bar{\mathfrak{h}}_3) \bullet \bar{\mathbf{s}}_2 \bullet \bar{\mathbf{s}}_3^*] \parallel_F^2$

From Table II, the data at each sub-carrier (tone) can be decoded separately, rather than jointly. For instance, the decoding metrics for data at the k-th sub-carrier, for $k = 1, \ldots, N_D$, in the MB-OFDM symbol $\bar{\mathbf{s}}_1$ are

$$s_{1,k} = \arg\min_{s\in\mathcal{C}} \Big[\Big|\big(\hbar_2\mathfrak{r}_2^* + \hbar_3\mathfrak{r}_3^* + \hbar_1^*\mathfrak{r}_1 + \hbar_4^*\mathfrak{r}_4\big) - s\Big|^2 + (-1 + \sum_{m=1}^{4} |\hbar_m|^2)|s|^2\Big] \quad (18)$$

where the complex space $\mathcal{C}$ denotes all potential possibilities that the PSK- or QAM-symbol s can take.

From Table III, a pair of data at each tone can also be decoded separately. For example, the decoding metrics for data at the k-th sub-carrier in the MB-OFDM symbols $\bar{\mathbf{s}}_1$ and $\bar{\mathbf{s}}_4$ are

$$\begin{aligned}\langle s_{1,k}, s_{4,k}\rangle = \arg\min_{s_1,s_4\in\mathcal{C}^{N_D}} \Big(\sum_{m=1}^{4} |\hbar_m|^2\Big)(|s_1|^2 + |s_4|^2) + \\ 2Real[(-\hbar_1\mathfrak{r}_1^* - \hbar_2^*\mathfrak{r}_2 - \hbar_3^*\mathfrak{r}_3 - \hbar_4\mathfrak{r}_4^*)s_1] + \\ 2Real[(-\hbar_4\mathfrak{r}_1^* + \hbar_3^*\mathfrak{r}_2 + \hbar_2^*\mathfrak{r}_3 - \hbar_1\mathfrak{r}_4^*)s_4] + \\ 2Real[(\hbar_1\hbar_4^* - \hbar_2^*\hbar_3 - \hbar_2\hbar_3^* + \hbar_1^*\hbar_4)s_1 s_4^*]\end{aligned} \quad (19)$$

TABLE IV

SIMULATION PARAMETERS.

Parameter	Value
FFT and IFFT size	$N_{fft} = 128$
Data rate	320 & 480 Mbps
Convolutional encoder's rate	1/2
Convolutional encoder's constraint length	$K = 7$
Convolutional decoder	Viterbi
Decoding mode	Hard
Number of transmitted MB-OFDM symbols	1200
Modulation	8-PSK, 16-QAM, DCM
IEEE Channel model	CM1, 2, 3 & 4
Number of data subcarriers	$N_D = 100$
Number of pilot subcarriers	$N_P = 12$
Number of guard subcarriers	$N_G = 10$
Total number of subcarriers used	$N_T = 122$
Number of samples in ZPS	$N_{ZPS} = 37$
Total number of samples/symbol	$N_{SYM} = 165$
Number of channel realizations	100

Next, we consider the MIMO systems with 4 Tx antennas and N Rx antennas. Linear combinations of the received signals from N Rx antennas are used to decode the transmitted symbols. Therefore, the decoding metrics of the transmitted symbol vectors can be deduced simply by replacing $\bar{\mathfrak{h}}_m$, for $m = 1, \ldots, 4$, in Tables II and III by the term $\sum_{n=1}^{N} \bar{\mathfrak{h}}_{m,n}$. Similar to MISO systems, each data point in S_{4a} (a pair of data points in S_{4b}) can be separately decoded. As a result, the decoding metrics for data points at the k-th sub-carrier can be deduced simply by substituting $\hbar_m$ in (18) and (19) by $\sum_{n=1}^{N} \hbar_{m,n}$.

IV. SIMULATION RESULTS

To examine the performance of the QOSTFC, we ran several Monte-Carlo simulations for the conventional MB-OFDM without STFCs, the OSTFC $\mathbf{S}_{4a}$ in (16), and the QOSTFC $\mathbf{S}_{4b}$ in (17). Each run of simulations was carried out with 1200 MB-OFDM symbols. One hundred channel realizations of each IEEE 802.15.3a channel model (CM 1, 2, 3 and 4) were considered for the transmission of each MB-OFDM symbol. In simulations, SNR is defined to be the signal-to-noise ratio (dB) per sample in a MB-OFDM symbol (consisting of 165 samples), at each Rx antenna. It means that, at a certain Rx antenna, SNR is the subtraction between the total power (dB) of the received signal corresponding to the sample of interest and the power of noise (dB) at that Rx antenna. To fairly compare the error performance of MB-OFDM systems with and without STFCs, the average power of the signal constellation points in the STFC MB-OFDM system is scaled down by a factor of 1/3 for $\mathbf{S}_{4a}$ and 1/4 for $\mathbf{S}_{4b}$. Thereby, the *same average transmission power* from all Tx antennas at a certain time can be achieved for three cases: conventional MB-OFDM without STFCs, and the two order-4 STFC MB-OFDM systems. The simulation parameters are listed in Table IV.

Figs. 2 and 3 compare the error performance of the conventional MB-OFDM, $\mathbf{S}_{4a}$, and $\mathbf{S}_{4b}$. It is noted that a suitable modulation scheme is selected for each MB-OFDM system

in order to achieve the *same data rate*. In particular, 8-PSK modulation is selected for the conventional MB-OFDM and for the $\mathbf{S}_{4b}$-QOSTFC MB-OFDM, while 16-QAM modulation is chosen for the $\mathbf{S}_{4a}$-OSTFC MB-OFDM. Thereby, all three systems have the same data rate of 480 Mbps. We can realize that at $SNR > 4$ dB, $\mathbf{S}_{4b}$ performs better than $\mathbf{S}_{4a}$. The more dispersive the UWB channel is, the better the code $\mathbf{S}_{4b}$ (over $\mathbf{S}_{4a}$) is. At $SNR < 4$ dB, $\mathbf{S}_{4a}$ performs better than $\mathbf{S}_{4b}$, however the advantage is negligible.

The reasons behind this error performance advance, though $\mathbf{S}_{4b}$ possesses half diversity of $\mathbf{S}_{4a}$, are due to the transmission power constraint and the data rate constraint. The use of a higher modulation scheme for $\mathbf{S}_{4a}$ (to have the same data rate) and the down-scaling of the signal constellation energy (to guarantee the power condition) cause a significant reduction of the Euclidean distance between the closest points in the signal constellation, which results in a higher BER for $\mathbf{S}_{4a}$, compared to that of $\mathbf{S}_{4b}$.

Figs. 4 and 5 show that an improvement of at least 6 dB can be achieved by $\mathbf{S}_{4b}$, compared to the conventional MB-OFDM system, at $BER = 10^{-4}$ with the data rate 320 Mbps, QPSK modulation/demodulation scheme, and with 1 or 2 Rx antennas. Similarly, Figs. 6 and 7 present the improvement of at least 3.1 dB achieved by $\mathbf{S}_{4b}$, compared to the conventional MB-OFDM system, in the case of DCM modulation/demodulation scheme.

V. Conclusions

In this paper, we have analyzed the implementation of order-4 QOSTFCs in our proposed STFC MB-OFDM UWB systems. Although only half diversity can be achieved, the order-4 QOSTFCs provide a full rate and considerably better error performance, compared to the rate-3/4, full diversity OSTFCs at SNRs greater than 4 dB. For lower SNRs, the performance of the OSTFC and of the QOSTFC are almost the same. Thus, it can be concluded that, for STFC MB-OFDM UWB, QOSTFCs might be better than OSTFCs, with the penalty of higher decoding complexity, though both QOSTFCs and OSTFCs have relatively simple decoding complexity.

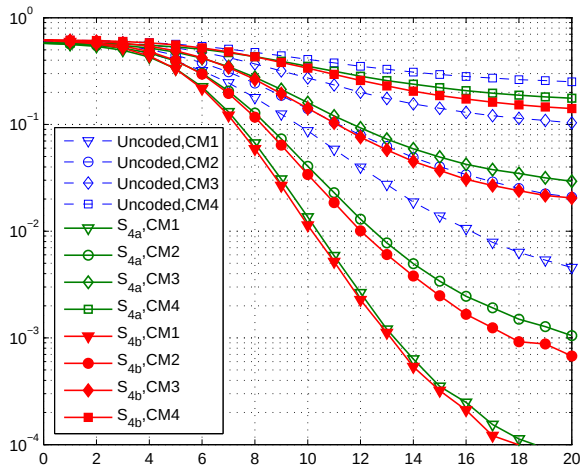

Fig. 2. STFC S_{4a} vs. QOSTFC S_{4b} with 1 Rx antenna and bit rate 480 Mbps.

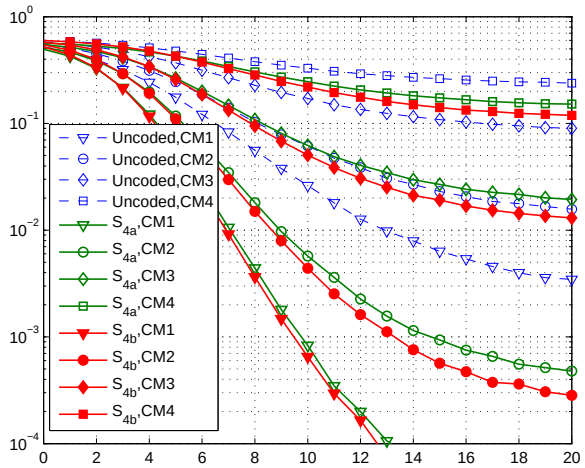

Fig. 3. STFC S_{4a} vs. QOSTFC S_{4b} with 2 Rx antennas and bit rate 480 Mbps.

Acknowledgment

L. C. Tran would like to thank the Alexander von Humboldt (AvH) Foundation, Germany, for its support of this work in form of a postdoctoral research fellowship.

References

[1] A. Batra et al., "Multiband OFDM physical layer specification," *WiMedia Alliance*, Release 1.1, July 2005.

[2] I. E. Telatar, "Capacity of multi-antenna Gaussian channels," *European Trans. Telecom.*, vol. 10, no. 6, pp. 585–595, 1999.

[3] G. J. Foschini and M. J. Gans, *On limits of wireless communications in a fading environment when using multiple antennas*, vol. 6 of *3*, Wireless Personal Communications, Printed in the Netherlands, Mar. 1998.

[4] S. M. Alamouti, "A simple transmit diversity technique for wireless communications," *IEEE J. Select. Areas Commun.*, vol. 16, no. 8, pp. 1451 – 1458, Oct. 1998.

[5] V. Tarokh, N. Seshadri, and A. R. Calderbank, "Space-time codes for high data wireless communications: performance criterion and code construction," *IEEE Trans. Inform. Theory*, vol. 44, no. 2, pp. 744 – 765, Mar. 1998.

[6] V. Tarokh, H. Jafarkhani, and A. R. Calderbank, "Space-time blocks codes from orthogonal designs," *IEEE Trans. Inform. Theory*, vol. 45, no. 5, pp. 1456 – 1467, July 1999.

[7] L. C. Tran, T. A. Wysocki, A. Mertins, and J. Seberry, *Complex Orthogonal Space-Time Processing in Wireless Communications*, Springer, New York, USA, 2006.

[8] X.-B. Liang, "Orthogonal designs with maximal rates," *IEEE Trans. Inform. Theory*, vol. 49, no. 10, pp. 2468–2503, Oct. 2003.

[9] Y. Gong and K. B. Letaief, "Space-time-frequency coded OFDM for broadband wireless communications," *Proc. IEEE Global Telecommunications Conference GLOBECOM '01*, vol. 1, pp. 519–523, Nov. 2001.

[10] A. F. Molisch, M. Z. Win, and J. H. Winters, "Space-time-frequency (STF) coding for MIMO-OFDM systems," *IEEE Commun. Lett.*, vol. 6, no. 9, pp. 370–372, Sept. 2002.

[11] Z. Liu, Y. Xin, and G. B. Giannakis, "Space-time-frequency coded OFDM over frequency-selective fading channels," *IEEE Trans. Sign. Process.*, vol. 50, no. 10, pp. 2465–2476, Oct. 2002.

[12] M. Fozunbal, S. W. McLaughlin, and R. W. Schafer, "On space-time-frequency coding over MIMO-OFDM systems," *IEEE Trans. Wireless Commun.*, vol. 4, no. 1, pp. 320–331, Jan. 2005.

[13] W. Su, Z. Safar, and K. J. R. Liu, "Towards maximum achievable

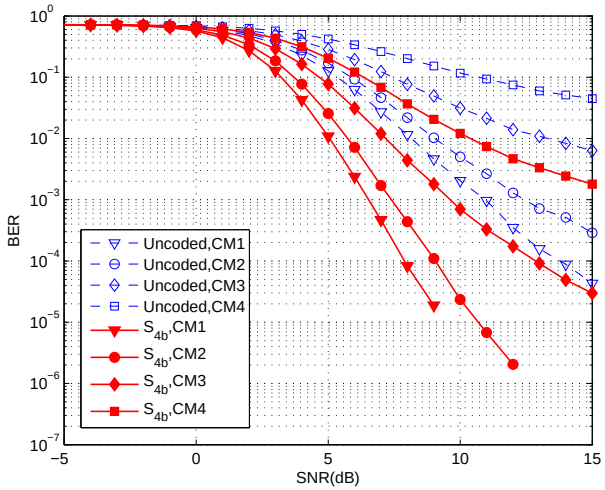

Fig. 4. QOSTFC S_{4b} with 1 Rx antenna, QPSK modulation/demodulation, and data rate 320 Mbps.

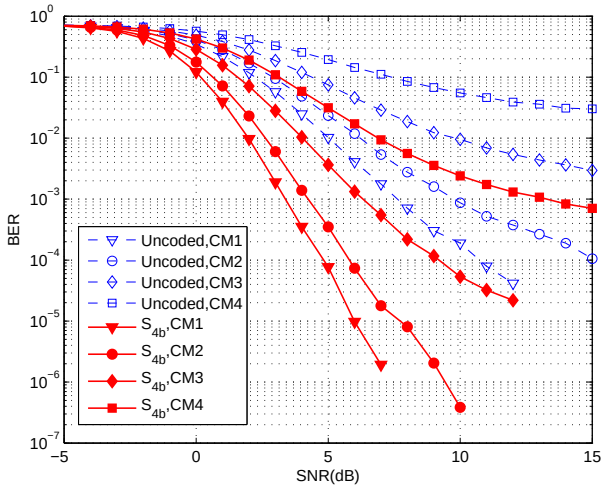

Fig. 5. QOSTFC S_{4b} with 2 Rx antennas, QPSK modulation/demodulation, and data rate 320 Mbps.

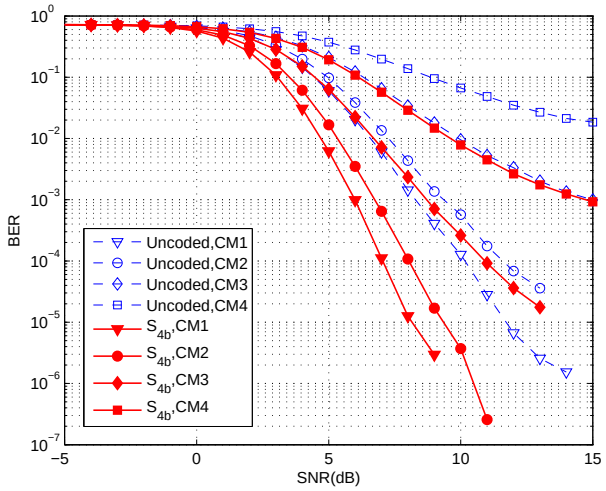

Fig. 6. QOSTFC S_{4b} with 1 Rx antenna, DCM modulation/demodulation, and data rate 320 Mbps.

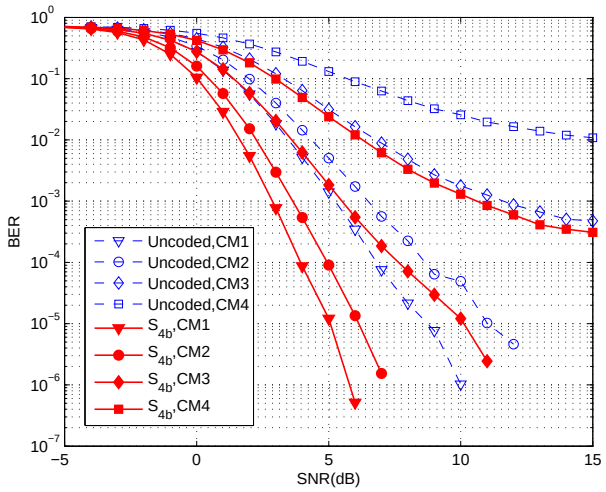

Fig. 7. QOSTFC S_{4b} with 2 Rx antennas, DCM modulation/demodulation, and data rate 320 Mbps.

diversity in sapce, time, and frequency: performance analysis and code design," *IEEE Trans. Wireless Commun.*, vol. 4, no. 4, pp. 1847–1857, July 2005.

[14] T.-H. Tan and K.-C. Lin, "Performance of space-time block coded MB-OFDM UWB systems," *Proc. 4th Annual Communication Networks and Services Research Conference (CNSR'06)*, pp. 323 – 327, May 2006.

[15] W. P. Siriwongpairat, W. Su, M. Olfat, and K. J. R. Liu, "Multiband-OFDM MIMO coding framework for UWB communication systems," *IEEE Trans. Signal Process.*, vol. 54, no. 1, pp. 214 – 224, Jan. 2006.

[16] J. Hou and M. H. Lee, "High rate ultra wideband space time coded OFDM," *Proc. 58th IEEE Veh. Technol. Conf. VTC 2003 - Fall*, vol. 4, pp. 2449–2451, Oct. 2003.

[17] J. Wang, G. Zhu, and J. Jin, "Optimal power allocation for space-time coded OFDM UWB systems," *Proc. IEEE Int. Conf. Wireless Communications, Networking and Mobile Computing WCNM.2005*, vol. 1, pp. 189 –192, Sept. 2005.

[18] J. Foerster et. al., "Channel modelling sub-committee report final," *IEEE P802.15 Working Group for Wireless Personal Area Networks (WPANs), IEEE P802.15-02/490r1-SG3a*, Oct. 2005.

[19] L. C. Tran and A. Mertins, "Space-time-frequency code implementation in MB-OFDM UWB communications: design criteria and performance," *submitted to IEEE Trans. Wireless Commun.*, Aug. 2007.

[20] Y. Viniotis, *Probability and random processes for electrical engineers*, McGraw-Hill, Printed in Singapore, 1998.

[21] H. Jafarkhani, "A quasi-orthogonal space-time block codes," *IEEE Trans. Commun.*, vol. 49, no. 1, pp. 1 – 4, Jan. 2001.

[22] A. Batra et al., "Multi-band OFDM physical layer proposal for IEEE 802.15 task group 3a," *IEEE P802.15-04/0493r1*, Sept. 2004.

[23] L. C. Tran, T. A. Wysocki, J. Seberry, A. Mertins, and S. A. Spence, "Generalized Williamson and Wallis-Whiteman constructions for improved square order-8 CO STBCs," *Proc. 16th IEEE Int. Symp. Personal Indoor and Mobile Radio Communications PIMRC'05*, vol. 2, pp. 1155 – 1159, Sept. 2005.

[24] L. C. Tran, J. Seberry, B. J. Wysocki, T. A. Wysocki, T. Xia, and Y. Zhao, "Two new complex orthogonal space-time codes for 8 transmit antennas," *IEE Electronics Lett.*, vol. 40, no. 1, pp. 55–56, Jan. 2004.

[25] V. Tarokh, H. Jafarkhani, and A. R. Calderbank, "Space-time block coding for wireless communications: performance results," *IEEE J. Select. Areas Commun.*, vol. 17, no. 3, pp. 451 – 460, Mar. 1999.

[26] O. Tirkkonen and A. Hottinen, "Square-matrix embeddable space-time blocks codes for complex signal constellations," *IEEE Trans. Inform. Theory*, vol. 48, no. 2, pp. 384 – 395, Feb. 2002.